Addressing Lubrication Challenges in Extreme Conditions Experienced in Subtractive Processes in Additive-Subtractive Hybrid Manufacturing (ASHM) of AISI H13

Hiva Hedayati and Maryam Aramesh *

Posted Date: 7 April 2025

doi: 10.20944/preprints202504.0560.v1

Keywords: ASHM; AISI H13; soft metal coating; lubrication in extreme conditions

 doi:10.20944/preprints202504.0560.v1

Article

Addressing Lubrication Challenges in Extreme Conditions Experienced in Subtractive Processes in Additive-Subtractive Hybrid Manufacturing (ASHM) of AISI H13

Hiva Hedayati and Maryam Aramesh *

Department of Mechanical Engineering, McMaster University, 1280 Main Street West, Hamilton, ON L8S 4L7, Canada

* Correspondence: arameshm@mcmaster.ca

Abstract: In additive subtractive hybrid manufacturing (ASHM), the combination of machining and additive processes in a single operation combines the benefits of both processes and thus enables the creation of high-quality complex parts. However, this method presents various challenges, particularly during the subtractive or machining steps. The machinability of parts produced through additive manufacturing is often low due to different factors such as high residual stresses and the presence of fine, hard microstructures. Furthermore, in ASHM intermediate heat treatments is not possible which results in subsequent increase in hardness of the printed workpiece material. Additionally, cutting fluids are unsuitable for controlling temperature and friction in ASHM because printing and machining occur simultaneously in the machine. The cutting fluid can contaminate the build environment, affecting layer adhesion and thus being detrimental to the printing operation. This study investigates the use of novel soft metallic lubricant coatings in ASHM, as a substitute for conventional fluid lubricants to address the lubrication challenges in the machining step. The novel proposed coating primarily serves as a lubricating layer between the tool and the workpiece material and provides an effective alternative to cutting fluids. The research aims to assess the effectiveness of these lubricant coatings in improving the surface integrity of additively manufactured parts, exploring a new way of machining without traditional fluid lubricants which is vital for the advancement of ASHM.

Keywords: ASHM; AISI H13; soft metal coating; lubrication in extreme conditions

1. Introduction

Additive manufacturing has come a long way since 1987, when one of the first additive manufacturing methods was introduced. Known as stereolithography (SL), the method was initially limited to certain polymers. Nevertheless, the invention of SL opened new opportunities for creating much more complex parts [1]. Since its development, additive manufacturing (AM) has facilitated the production of complex components that were challenging to manufacture with traditional methods. The first additively manufactured part using metal alloy powder was reported in 1990, utilizing selective laser sintering (SLS) technology. Today, the process for metals is more commonly referred to as selective laser melting (SLM), as it achieves full melting of the metal powder [2]. Most current metal additive manufacturing systems use powder bed fusion. In this process, thin layers of powder are spread on a build plate, and an energy source (laser or electron beam) fuses the powder according to the desired design. After each layer is completed, a new layer of powder is added, repeating the process until a 3D part is formed. Powder bed fusion may also be known as selective laser sintering (SLS), selective laser melting (SLM), direct metal laser sintering (DMLS), direct metal laser melting (DMLM), or electron beam melting (EBM) [3]. Despite advancements in additive manufacturing, challenges remain, such as unsatisfactory surface roughness and internal defects like porosity, cracks, and residual stress between layers. These defects can negatively impact the

 doi:10.20944/preprints202504.0560.v1

microstructure and mechanical properties of the parts. As a result, a series of post-processing operations are often necessary to ensure the quality of the final product, enhance mechanical properties, and address defects from the additive manufacturing process. Post-processing is essential to prevent distortions caused by rapid cooling and the remelting of the bottom layer during the deposition and solidification of subsequent layers, leading to thermal cycles in the final part upon completion of printing.

These operations include stress relief, removal of the part and support structures, and machining [4,5]

There are other challenges with creation of accurate and flexible designs for components, such as conformal cooling channels, and the fabrication of parts without the need for support structures, and also in finishing or machining certain regions of the final printed parts, which are often inaccessible to conventional machining tools.

To address these challenges mentioned above, additive subtractive hybrid machine (ASHM) was introduced in 2014, integrating additive manufacturing with 5-axis machining. This method represents a significant advancement in the AM sector and offers multiple benefits. One of the primary advantages is its effectiveness in machining areas that are challenging to machine afterwards. Moreover, it allows for the removal of support structures, potentially using a multi-axis system or jointed-arm robots, also mitigating the requirement for additional processing stages [6]. Furthermore, ASHM has demonstrated effectiveness in reducing additional movements by maintaining the part's clamping position throughout the process. Consequently, this leads to a decrease in both the time required for product production and material waste [7].

Despite all the benefits of ASHM technology, there are still some challenges associated with additive and machining processes. Each process presents its own specific challenges that require individual attention, along with additional issues arising from integrating these two methods in a single machine, such as the cutting fluid-laser integration. In this paper, we introduce a novel solution that addresses the problems associated with both machining and the joint cutting fluid-laser integration simultaneously.

In general, machining additive manufactured (AM) parts can be more challenging than machining wrought parts due to factors such as anisotropy in mechanical properties and higher strength and hardness of the material. These characteristics result in significantly increased cutting forces, leading to elevated tool wear and failure, which can adversely affect the surface integrity of the machined parts [8].

Additionally, in ASHM, the use of cutting fluids presents challenges and is often unsuitable, as they can interfere with the simultaneous printing operation. Even if cutting fluids could be implemented, they might cause faster cooling rates, resulting in a more inhomogeneous microstructure that is not desirable. Furthermore, removing excessive cutting fluid from parts by blowing them off, a common practice by some manufacturers, poses significant challenges as the presence of metal powder can create fire and explosion hazards [9]

On the other hand, dry machining of AM parts requires highly wear and temperature-resistant tools, which can be quite expensive. Even with such tools, extreme conditions of friction, temperature and pressure makes machining of difficult-to-cut AM materials, such as AM H13 tool steel very challenging without lubricants.

Considering the challenges associated with liquid lubricants in these processes, this research introduces a new class of solid lubricant coatings that can be used for dry machining of AM AISI H13 materials. These coatings have demonstrated effectiveness under the extreme conditions encountered during machining, providing an alternative solution for ASHM processes.

In general, solid lubricants exhibit a high degree of thermal stability, making them suitable for demanding operational conditions. This implies that, owing to their intrinsic limited elasticity and lower tendency to evaporate, the frequency of reapplication can be minimized. Studies have indicated that solid lubricants are efficacious in lowering friction and wear, thereby enhancing the operational efficiency and extending the service life of tools. However, our previous review study

 doi:10.20944/preprints202504.0560.v1

found that most solid lubricants used in machining, such as MoS2 and graphite, need to be applied in powder form and are carried with water or oil-based lubricants[10]. Although methods like MQSL are employed to deliver these lubricants and reduce fluid consumption, they remain suboptimal for processes like AHSM.

One of the categories of solid lubricants includes soft metals such as Ag and Au. Soft metals have been used as solid lubricants, mainly in engine bearings. However, their performance has been limited by their melting point, and they have never been used as lubricants in machining, where extreme temperatures and pressures occur. Aramesh recently introduced soft metals as solid lubricants in machining. In their previous work, they observed that specific metallic alloys, such as Al-Si alloys, can be used as solid lubricants in machining operations with significant benefits, including reduced friction, chipping, workpiece microstructural alterations, and improved surface integrity and productivity [11,12]

This new discovery could significantly benefit the subtractive aspect of ASHM by eliminating the need for cutting fluids and reducing friction under harsh conditions, resulting in improved surface integrity and lower failure rates. This study seeks to enhance this process by exploring the impact of applying this new class of solid, soft metal lubricant coatings on inserts used in the ASHM of AISI H13 material.

Due to the lack of access to an ASHM machine, we mimicked the process in this study by machining a part that was additively manufactured in our previous work using the Laser Powder Bed Fusion (LPBF) technique, followed by a machining step with our new coated tools. For comparison, the results were evaluated against those from dry and wet machining using uncoated tools. The next sections provide a brief overview of the additive manufacturing process of AISI H13 using the LPBF method, followed by detailed machinability analyses that include tool and workpiece characterizations. These sections focus on understanding how the soft metal impacts the surface integrity of the workpiece, which is the main challenge for ASHM. The results include analyses of machining forces, surface integrity, and chip formation. Phase quantification and characterization techniques, such as electron backscatter diffraction (EBSD), X-ray diffraction (XRD), and other methods, are employed for detailed surface characterization.

2. Experimental Procedures

2.1. Laser Powder Bed Fusion (LPBF) Samples

The fabrication of the AISI H13 workpiece has been previously conducted in our institution, all details of this process can be found in the previous publications [13]. To briefly explain, AISI H13 test samples were made using the LPBF process on an EOS M280 machine (Germany, Krailling) equipped with a Yb-fiber laser system delivering a maximum power of 400 W. A high-purity atmosphere of nitrogen gas was applied to reduce the oxygen content in the build chamber to less than 0.1%, hence reducing the oxidation during the melting process. The chemical composition of the powder was determined using ICP-OES digestion and the results were validated against the ASTM standard for the alloy's chemical composition, as shown in Table 1.

Table 1. Comparison of chemical composition of AISI H13 powder according to ASTM and ICP.

Element (wt.%)	Cr	Mo	Si	V	Mn	C	Fe
ASTM-A681	4.75–5.5	1.10–1.75	0.8–1.25	0.8–1.2	0.2–0.6	0.32–0.45	Bal.
ICP-OES	5.27	1.34	1.08	0.97	0.40	0.39	Bal.

AISI H13 tool steel has a propensity to crack, so the build-plate was preheated to 200 °C to eradicate the possibility of crack development in the as-built parts. The samples were fabricated directly on the build plate in the direction of the thickness with no support structures and underwent no post-processing procedures. A constant layer thickness of 40 μm, in tandem with a 67° rotation of

 doi:10.20944/preprints202504.0560.v1

scanning pattern between subsequent layers and a stripe scanning strategy with a width of 10 mm, was maintained during the LPBF process. Machining set-up and parameters.

Machining experiments were conducted using an FX-5 CNC three-axis vertical milling machine, equipped with a 7.5 kW power capacity and capable of reaching a maximum spindle speed of 28,000 rpm. For the tests, the machine's tool holder, designed to accommodate two tool inserts, was fitted with a single insert. This approach was adopted to facilitate precise wear measurement of each tool. The radius of the tool holder/insert, defined as the distance from the insert's cutting edge to the center of the tool holder, was set at 9.525 mm. Furthermore, the specified angles for the insert included a clearance angle of 10°, an axial rake angle of 14.73°, and a radial rake angle of -9.805°.

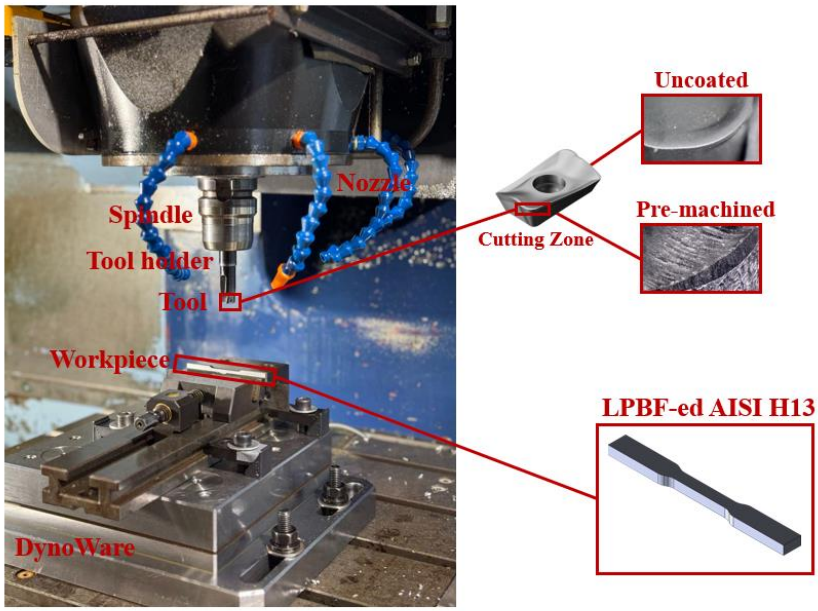

Figure 1. Machining setup for the experiment. The uncoated tool was treated for pre-machining, which is illustrated in the cutting zone region. .

2.2. New Coating Process; Pre-Machining

The lubricant coating used in this study is Al-Si with 8% silicon content, applied using the novel pre-machining technique instead of traditional Physical Vapor Deposition (PVD) for coating the tools. This method has shown superior machining results compared to PVD and is significantly more cost-effective, environmentally friendly, quick, and easy to apply [14].

In the pre-machining process, as proposed previously by Aramesh [11], a layer of the Al-Si target material is deposited on the tool by machining the target material for a few seconds. Due to patent protection, further details, including the cutting regime and parameters, cannot be disclosed at this time. Details of the process are being withheld for a future publication. The resulting deposited layer on the tool acts mainly as a solid lubricant, reducing friction during the actual machining of the workpiece material.

In this investigation, the cutting conditions for machining the AISI H13 workpieces were purposely pushed to their realistic limits to examine the performance of the suggested treatment under extreme conditions. A very rapid cutting speed of 300 m/min and a comparatively low feed rate and depth of cut were used, as shown in Table 2. given the very small size of additively manufactured samples, several cutting speeds were investigated to determine the speed at which considerable wear results could be obtained given the short cutting length. For comparison, machining tests were also conducted using an uncoated tool under both dry and wet conditions, with industry-standard benchmark cutting fluids. New tools were used for all tests, the cutting conditions were kept consistent, and the same cutting length of 30 mm was maintained.

 doi:10.20944/preprints202504.0560.v1

Table 2. Cutting condition parameters and settings used for machining of AISI H13.

Parameter	Setting	Unit
Machine	Matsuura Fx-5	
Machining condition	Milling-Dry	
Cutting speed	300	m/min
Tool type	Indexable shoulder milling	
Tool ID	R390-11 T3 02E-KM H13A	
Tool holder diameter	19.05	mm
No. of teeth	1	
Feed per tooth	0.15	mm
Cutting length	30	mm
Depth of cut	1	mm
Radial /depth of cut	1	mm

Tool wear and cutting forces were monitored after each pass; three passes were performed on each tool. Following the machining tests, machinability investigations, including wear surface analyses, microstructural and tribological studies of the worn surfaces, and surface integrity analyses of the machined surfaces, were performed. Cutting forces were quantified using a Kistler 9255B piezoelectric dynamometer, which provides three-channel force measurements (Fx, Fy, Fz). The dynamometer's output signals were relayed to a data acquisition system via a Kistler 5167A multi-channel amplifier. These signals were then converted into numerical values using Dyno Ware software for analysis. The surface texture, characterized by the parameters Sa and Sz, of the machined surfaces, along with the roughness of the worn area on the tool's flank face, was evaluated employing Bruker Alicona InfiniteFocus G5 and Keyence VHX-5000 microscopes. These instruments are equipped with focus variation technology, enabling precise measurement and analysis of surface characteristics. At least three measurements were taken to ensure consistency in the readings. To assess the characterization of the workpieces, a Tescan Vega II LSU scanning electron microscope (SEM) was used with a 30 kV accelerating voltage and a JEOL JSM-7000F was used with a 20 kV accelerating voltage, a working distance of 15 mm, and a step size of 70 nm. Inverse pole figures, KAM maps, and phase maps were processed using Aztec EDS/EBSD Crystal software. Residual stresses on the surface of the workpiece were measured using X-ray diffraction (XRD) with LEPTOS software. Cobalt X-ray radiation with a wavelength of 1.79 Å (Kα) was employed to assess the residual stress of the machined surface.

3. Results and Discussion

3.1. Machining Results

3.1.1. Tool Wear Readings

Tool wear readings acquired from the Keyence showed a decrease in tool wear, as illustrated in Figure 2. This decrease can be attributed to the function of Al-Si as a lubricious coating, which resulted in an approximately 50% reduction in tool wear.

Please note that since the machining was performed on additively manufactured parts, obtaining full tool wear curves was not possible due to the material's limitations. However, it is well known that the running-in stage in machining significantly impacts overall results, and better running-in performance leads to enhanced overall performance. Our previous results demonstrated a significant improvement in overall tool life due to enhanced running-in performance when machining Inconel 718. Similar trends are expected with AISI H13, given the noteworthy 50% improvement, higher than any previous results, observed during the first pass.

 doi:10.20944/preprints202504.0560.v1

Figure 2. Tool wear readings under the two conditions of Uncoated-Dry and Coated-Dry.

3.1.2. Force Analysis

The force results are presented in Figure 3. As the figure shows, there was a significant force reduction when using Al-Si lubricant coating. After applying the coating, the average force was reduced by approximately 65% compared to dry machining. To evaluate the effectiveness of the lubricant coating against benchmark liquid lubricants, an uncoated carbide tool used with flood liquid lubrication was tested using the same machining parameters. Force results depicted in Figure 3 show that the novel coated lubricant is comparable to, and even more effective than, liquid lubrication in flood applications, making it possible to eliminate the need for flood lubrication in the machining process.

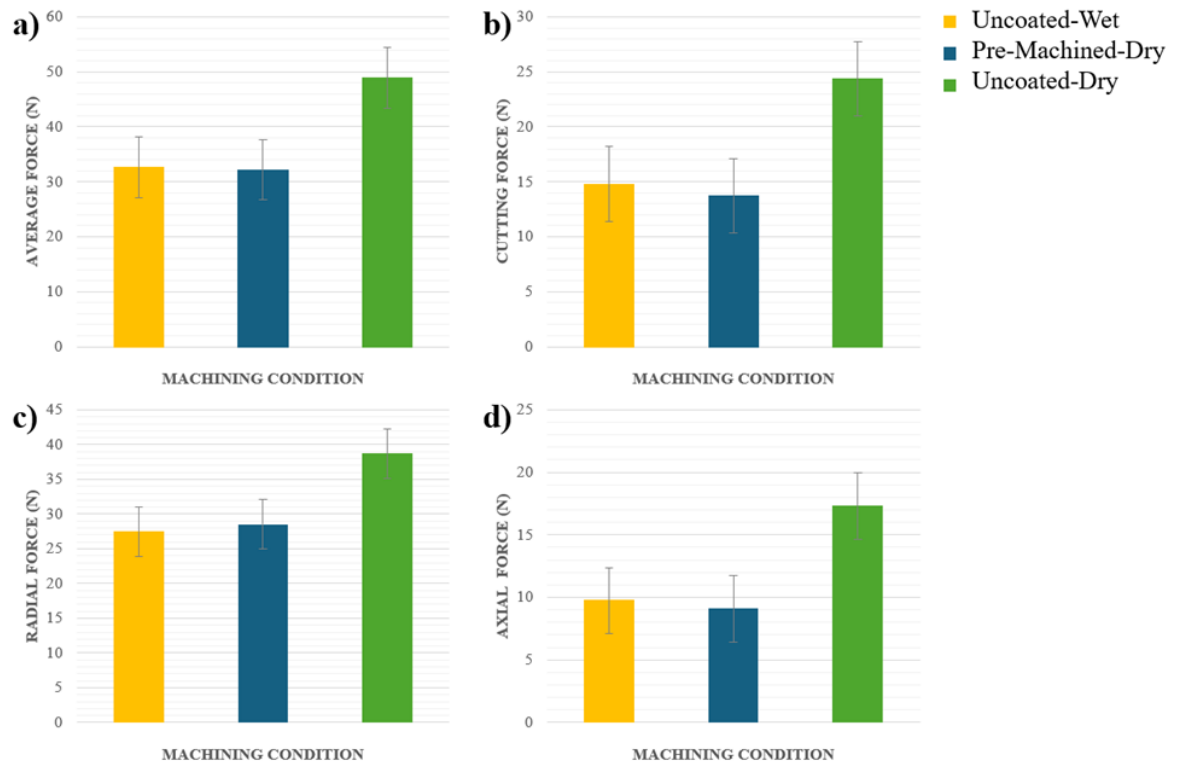

Figure 3. Force data of three conditions of Uncoated-Wet, Coated-Dry, and Uncoated-Dry at the cutting speed of 300 m/min: a) average machining force (b) cutting force, (c) radial force, (d) feed force.

 doi:10.20944/preprints202504.0560.v1

In Figure 3a, the average machining force of the Coated-Dry condition appears comparable to that of the Uncoated-Wet condition, often regarded as the conventional lubricated state for reducing machining forces. When comparing the cutting force based solely on Figure 3b, the Coated-Wet condition demonstrates marginally improved performance relative to the Uncoated-Wet condition. Moreover, there is a substantial reduction in force when compared to the Uncoated-Dry condition, aligning with the primary objective of this research, which is to achieve a force reduction of approximately 45%. The same trend is observed for radial force readings in Figure 3c and feed force readings in Figure 3d, with reductions of approximately 30% and 47%, respectively. The 47% reduction in feed force clearly proves the effectiveness of the lubricant coating in reducing friction during machining.

This reduction in forces can be attributed to the performance of Al-Si as a lubricant coating, resulting in lower friction, reduced contact pressure in the sticking zone under seizure conditions, and enhanced material flow due to Al-Si acting as a lubricious film [12]. Also, it is worth mentioning that Al-Si alloys are known to exhibit force-damping properties [15].

3.2. Surface Integrity Analysis

3.2.1. Surface Analysis

Surface Topography

To study the effect of force reduction on surface integrity of the machined parts, as the first step optical microscopy analyses were performed on surfaces machined with uncoated and tools coated with our solid lubricant coating using the Alicona InfiniteFocus G5. Due to material limitations and the small cutting lengths, the overall roughness values (Sa) were not significantly different. However, as shown in Figure 4-a, in general, the surface machined with our lubricant coating appears smoother with fewer irregularities. In contrast, as seen in Figure 4-b, more deep grooves are evident on the surface machined with an uncoated tool.

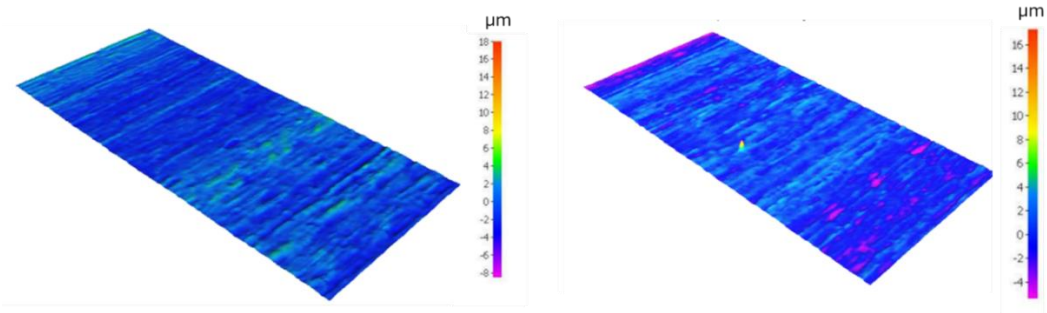

Figure 4. Surface quality machined with a) coated tool b) uncoated tool.

Surface Roughness

The presence of deeper grooves and higher irregularities are also reflected in corresponding roughness parameters of the two surfaces as illustrated in Figure 5. The results were obtained by averaging three measurements taken from three different areas. The average values and standard deviations for the surface machined with the uncoated tool were notably higher than those for the surface machined with our lubricant-coated tool. This suggests that using our lubricant coating during machining could reduce surface roughness, resulting in a smoother finish. This improvement could be attributed to reduced friction and sticking, contributing to better cutting flow.

 doi:10.20944/preprints202504.0560.v1

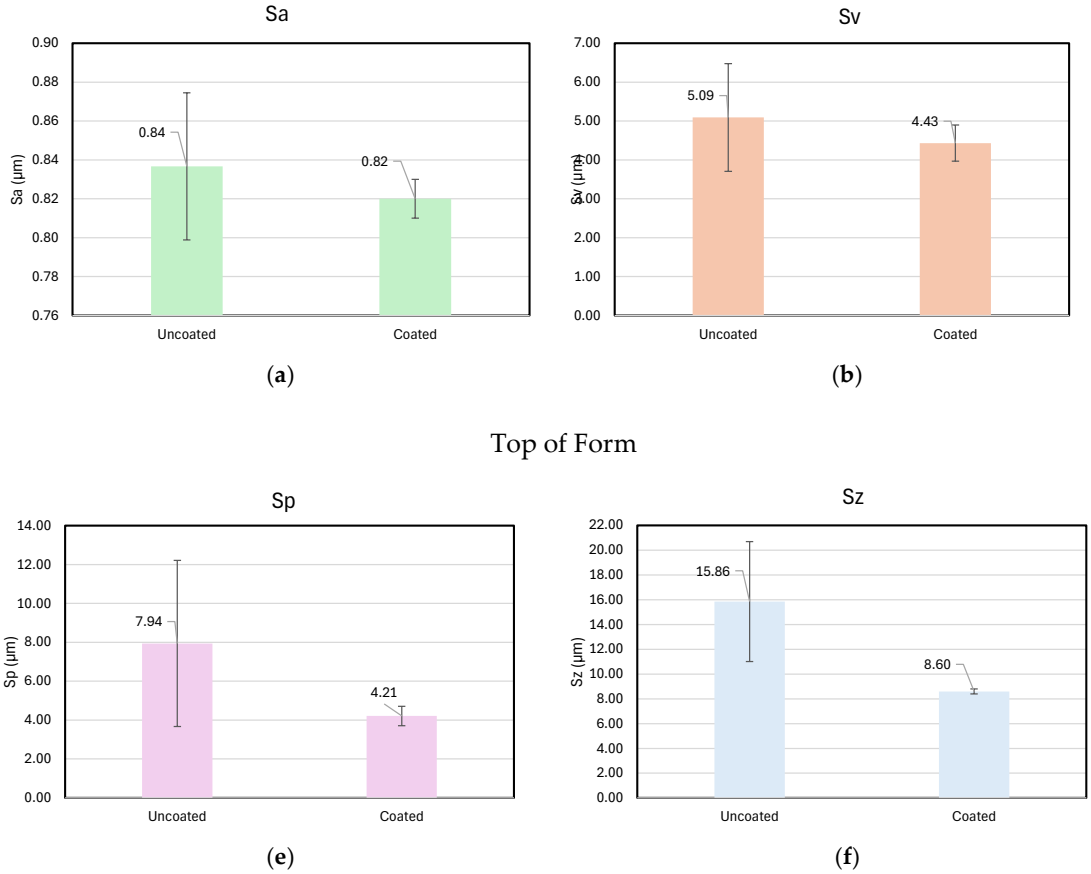

Figure 5. Measured roughness parameters for the two surfaces.

3.2.2. Sub-Surface Analysis

EBSD Analysis of Subsurfaces

For an in-depth surface integrity analysis and study the effect of our solid lubricant on reducing the microstructural evolution during machining, EBSD analyses were performed on the machined surfaces using our lubricant coated tools and uncoated tools and the results have been summarized in this section.

An schematic of the machined sample is shown in Figure 6. The region of interest and direction of cut are depicted in the picture.

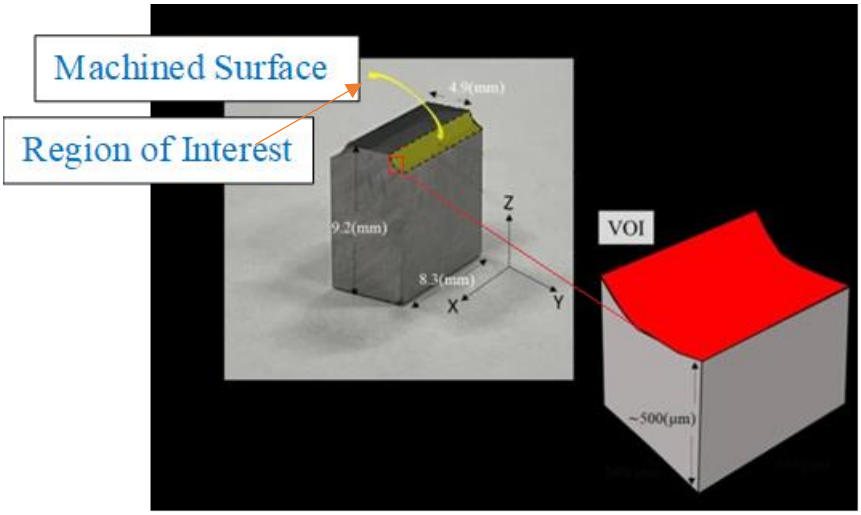

Figure 6. The schematic of the machined sample.

 doi:10.20944/preprints202504.0560.v1

Figure 7 displays the band contrast of machined samples using the 2 different tools: Uncoated and Al-Si coated tools in dry conditions. The microstructure of both samples appears to be predominantly martensitic, showing a transition to finer lath sizes closer to the machined surfaces. A high dislocation density is observed on the subsurface of the uncoated sample, appearing as a non-indexed region in EBSD [16–18]. The coated sample exhibits a thinner layer of severe deformity near the subsurface due to the less forces and stresses experienced, as seen in Figure 3, which resulted in a shallower affected zone on the machined surface [19].

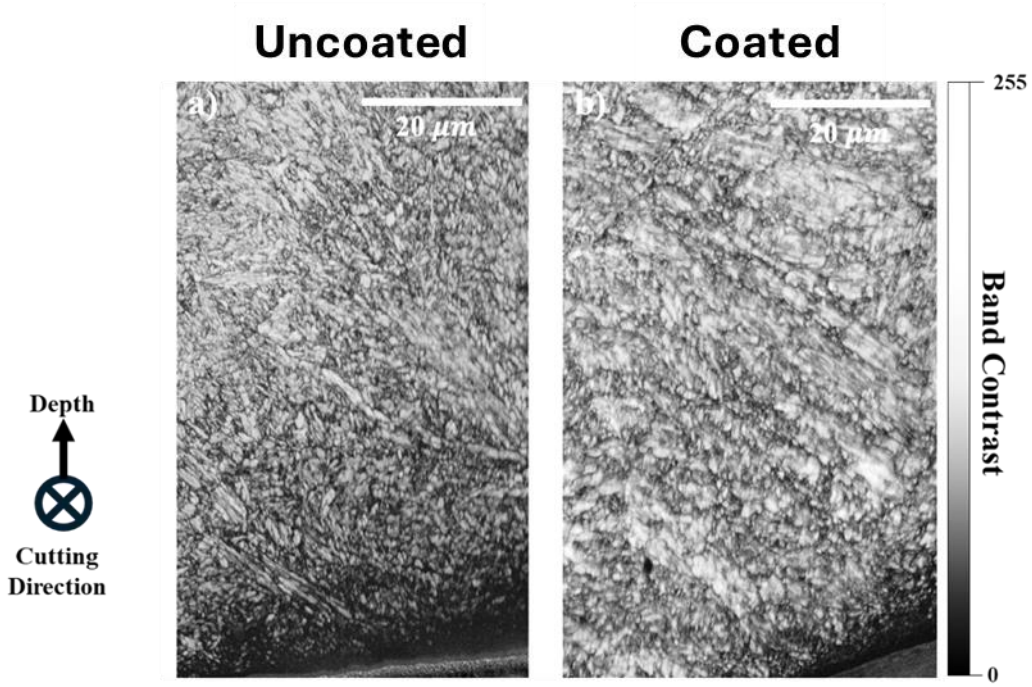

Figure 7. Band contrast maps of AISI H13-LPBFed sub surfaces. The cutting direction is illustrated in the figure and a depth direction is also provided. (a) Uncoated sample and (b) Coated sample.

Figure 8 presents the kernel average misorientation (KAM) maps for both the uncoated and coated samples. These maps, which illustrate the distribution of localized strain throughout the microstructure based on misorientation angles, reveal that strain localization is significantly more pronounced near the surface areas. The uncoated sample's strain appears to thicker beneath the surface and also more widespread into the core compared to the coated sample, where the strain is predominantly restricted to the subsurface. The observation of higher localized strain on the subsurface of the uncoated sample suggests that elevated cutting temperatures resulted in thermally induced damage and altered the strain distribution in the subsurface layer of the workpiece. The temperature increase during the cutting process can alter the material properties and affect the integrity of the subsurface, impacting its physical and mechanical characteristics [20].

 doi:10.20944/preprints202504.0560.v1

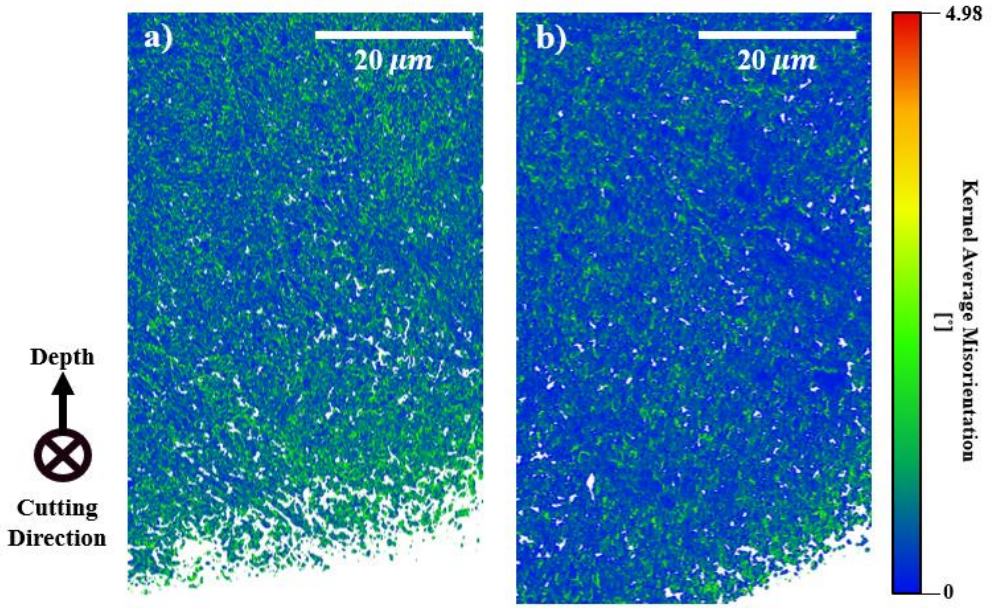

Figure 8. KAM map presenting strain distribution for (a) Uncoated-Dry and (b) Coated-Dry.

Figure 9a,b show the inverse pole figure (IPF) map of the machined sample along the machining direction. The surface generated using the lubricant coated tool demonstrates a more random crystallographic texture near the subsurface, which agrees with the pole figure results seen in Figure 9c,d. The maximum intensity of the pole figure is lower for the coated sample at 3.09, compared to the higher intensity of 8.39 for the uncoated sample. The degree of force applied during the machining process (Figure 3) seems to follow the observed textural changes, with stronger forces leading to a more pronounced cube component post-machining.

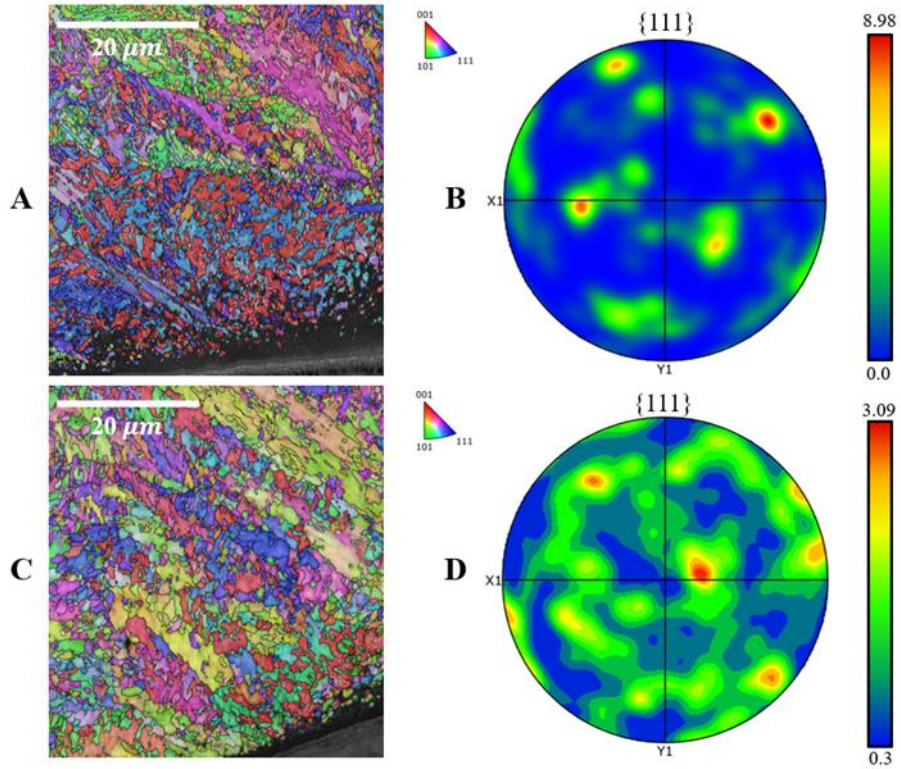

Figure 9. IPF maps and pole figures of AISI H13-LPBFed sub surfaces. (a) Uncoated-Dry IPF map, (b) Coated-Dry IPF map, (c) Uncoated pole figure, and (d) Coated pole figure.

XRD Analysis

 doi:10.20944/preprints202504.0560.v1

Supporting previous observations, XRD analysis was performed on the machined samples and the phase map and XRD results are shown in Figure 10. The results show the distribution of martensite phases within the retained austenite in the microstructures of both samples, revealing a slightly higher fraction of martensite in the uncoated sample specially close to the machined surface. This observation correlates with the greater intensity of the applied force in the uncoated sample. Stress-induced phase transformation during machining, where austenite transformed to martensite during machining of AISI has been reported before [21]. External stresses, particularly under uncoated dry conditions, during the post-machining of an additively manufactured part can encourage the transformation of retained austenite to martensite. Figure 10a shows that the coated dry sample contains 12% retained austenite, which is slightly higher than the 10.8% observed in the uncoated sample.

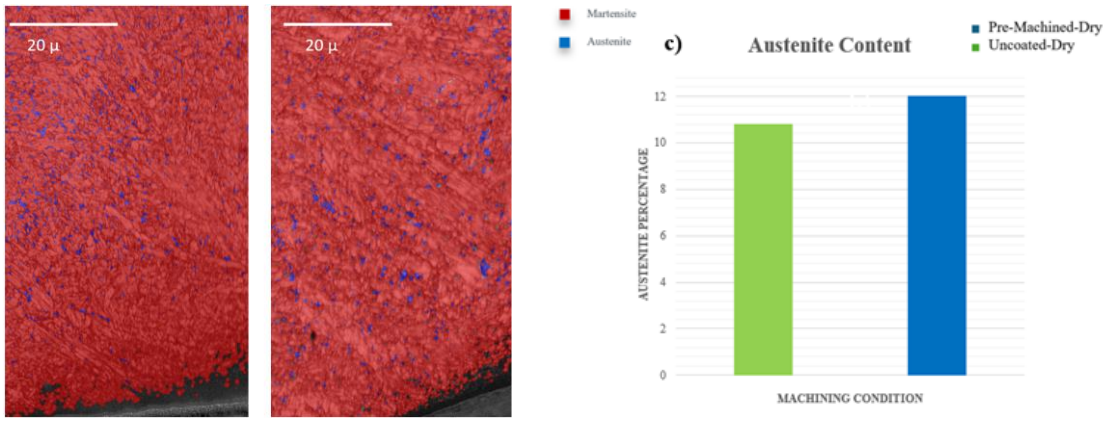

Figure 10. (a) EBSD phase map of Uncoated-Dry sample, (b) EBSD phase map of Coated-Dry sample, and (c) comparative analysis of retained austenite content in uncoated and Coated samples via XRD phase quantification.

4. Conclusions

This study aimed to enhance the ASHM process by applying a soft metal coating as a lubricant to replace cutting fluids and enable high-performance dry machining of additively manufactured AISI H13. The study investigated the impact of a soft metal coating (Al-Si) on the surface integrity of the final part by analyzing machining results and characterizing the final product using EBSD, SEM and XRD. Since we did not have access to an ASHM machine, to mimic the machining step in a ASHM process, we machined a laser powder bed-fused AISI H13 piece without heat treatment or any other post-processing The results were compared with an uncoated carbide tool as the objective of this study was to avoid cutting fluid and function under dry machining conditions.

It should be mentioned that this study was limited by a small sample size due to a shortage of materials for additive machining. Yet, a single pass on each sample showed significant alterations in the part's machinability and surface quality. The machinability results may change as the tool continues to wear and the contact area grows, and thus a future study with longer tests and a larger sample size is recommended to corroborate these findings. However, it is widely recognized that enhancing the running-in stage of machining leads to overall process improvements, a finding supported by our previous studies. In this current study, we achieved significant enhancement in the running-in stage, thus expecting an overall improvement of the process in longer cuts as well.

The noticeable improvements in machinability and surface integrity are presented as follows:

- Tool wear analysis indicated a significant 50% decrease in tool wear resulting from the presence of the Al-Si lubricant coating in the cutting zone.
- Force analysis indicated a notable decrease in cutting force, radial force, and axial force.
- Observations of surface roughness via SEM and advanced microscopy revealed a notable enhancement in surface texture and finish following the application of an Al-Si-coated tool. The

 doi:10.20944/preprints202504.0560.v1

treated surface exhibited a considerable reduction in the incidence of grooves and defects, implying a superior surface quality on the final part.

- EBSD maps were extracted to examine the integrity of the sub-surfaces under two specific conditions: coated and uncoated. The results aligned with the machining outcomes observed in this study. The band contrast map showed increased dislocation density on the subsurface of the uncoated sample, indicating significant deformation near the machined surface due to greater machining forces when using an uncoated tool, compared to the coated tool.
- The KAM map also demonstrated increased localized strain in the subsurface of the uncoated sample. Interestingly, the affected zone associated with the uncoated tool was not limited to the machined surface but also extended to the core.
- Analysis of the IPF maps and pole figures for the machined samples reveal that the coated-sample displayed a more random crystallographic texture near the subsurface, with a lower maximum intensity than the uncoated sample. This suggests that the force applied during the machining process influences textural changes, with higher forces resulting in more distinct textural patterns following machining.
- The phase map and XRD phase quantification results are also consistent with previous findings. The phase map (a qualitative phase measurement) revealed more austenite near the surface of the coated sample, which can be attributed to a lower transformation of austenite into martensite due to reduced stresses resulting from improved lubrication. The XRD analysis confirmed this observation as a quantitative measurement method.

In conclusion, our novel soft metal coating as a solid lubricant proves to be an effective solution for the subtractive part of the ASHM process. It allows for dry machining under the extreme conditions faced during the machining of additive parts, while maintaining the surface integrity of the workpiece which is a challenge often seen in traditional dry machining methods. Applying out novel solid lubricant coating improves machining performance and also helps ensure the quality of the final product, making our coated lubricant a valuable advancement in the ASHM process.

Acknowledgement: We would like to acknowledge Dr. Shahryar Asqardoust for acquiring EBSD maps and Dr. Morteza Narvan and Dr. Mo Elbestawi for providing AM fabricated parts to help us conduct this research. We would also like to thank the Natural Sciences and Engineering Research Council of Canada (NSERC) for funding this research.

References

1. T. Wohlers et al., "Wohlers Report 2022, History of Additive Manufacturing," Jan. 2022. doi: 10.13140/RG.2.2.23598.59203.
2. W. J. Sames, F. A. List, S. Pannala, R. R. Dehoff, and S. S. Babu, "The metallurgy and processing science of metal additive manufacturing," *International Materials Reviews*, vol. 61, no. 5, pp. 315–360, Jul. 2016, doi: 10.1080/09506608.2015.1116649.
3. W. E. King et al., "Laser powder bed fusion additive manufacturing of metals; physics, computational, and materials challenges," *Appl Phys Rev*, vol. 2, no. 4, p. 041304, Dec. 2015, doi: 10.1063/1.4937809.
4. O. Oyelola, P. Crawforth, R. M'Saoubi, and A. T. Clare, "Machining of Additively Manufactured Parts: Implications for Surface Integrity," *Procedia CIRP*, vol. 45, pp. 119–122, 2016, doi: 10.1016/j.procir.2016.02.066.
5. X. Peng, L. Kong, J. Y. H. Fuh, and H. Wang, "A Review of Post-Processing Technologies in Additive Manufacturing," *Journal of Manufacturing and Materials Processing*, vol. 5, no. 2, p. 38, Apr. 2021, doi: 10.3390/jmmp5020038.
6. S. Akula and K. P. Karunakaran, "Hybrid adaptive layer manufacturing: An Intelligent art of direct metal rapid tooling process," *Robot Comput Integr Manuf*, vol. 22, no. 2, pp. 113–123, Apr. 2006, doi: 10.1016/j.rcim.2005.02.006.

 doi:10.20944/preprints202504.0560.v1

7. L. Li, A. Haghighi, and Y. Yang, "Theoretical modelling and prediction of surface roughness for hybrid additive–subtractive manufacturing processes," *IISE Trans*, vol. 51, no. 2, pp. 124–135, Feb. 2019, doi: 10.1080/24725854.2018.1458268.
8. C. Zhang, D. Zou, M. Mazur, J. P. T. Mo, G. Li, and S. Ding, "The State of the Art in Machining Additively Manufactured Titanium Alloy Ti-6Al-4V," *Materials*, vol. 16, no. 7, p. 2583, Mar. 2023, doi: 10.3390/ma16072583.
9. M. Cortina, J. I. Arrizubieta, J. E. Ruiz, E. Ukar, and A. Lamikiz, "Latest Developments in Industrial Hybrid Machine Tools that Combine Additive and Subtractive Operations," *Materials*, vol. 11, no. 12, p. 2583, Dec. 2018, doi: 10.3390/ma11122583.
10. H. Hedayati, A. Mofidi, A. Al-Fadhli, and M. Aramesh, "Solid Lubricants Used in Extreme Conditions Experienced in Machining: A Comprehensive Review of Recent Developments and Applications," *Lubricants*, vol. 12, no. 3, p. 69, Feb. 2024, doi: 10.3390/lubricants12030069.
11. Maryam Aramesh, "Ultra soft cutting tool coatings and coating method," US20210129230A1, 2019
12. M. Aramesh, S. Montazeri, and S. C. Veldhuis, "A novel treatment for cutting tools for reducing the chipping and improving tool life during machining of Inconel 718," *Wear*, vol. 414–415, 2018, doi: 10.1016/j.wear.2018.08.002.
13. M. Narvan, " Laser Powder Bed Fusion of AISI H13 Tool Steel for Tooling Applications in Automotive Industry," McMaster University, Hamilton, 2021.
14. S. Montazeri, M. Aramesh, A. F. M. Arif, and S. C. Veldhuis, "Tribological behavior of differently deposited Al-Si layer in the improvement of Inconel 718 machinability," *The International Journal of Advanced Manufacturing Technology*, vol. 105, no. 1, pp. 1245–1258, 2019, doi: 10.1007/s00170-019-04281-1.
15. Q. G. Wang, "Microstructural effects on the tensile and fracture behavior of aluminum casting alloys A356/357," *Metallurgical and Materials Transactions A*, vol. 34, no. 12, pp. 2887–2899, Dec. 2003, doi: 10.1007/s11661-003-0189-7.
16. V. Javaheri et al., "Formation of nanostructured surface layer, the white layer, through solid particles impingement during slurry erosion in a martensitic medium-carbon steel," *Wear*, vol. 496–497, p. 204301, May 2022, doi: 10.1016/j.wear.2022.204301.
17. S. Wu, G. Liu, W. Zhang, W. Chen, and C. Wang, "Formation mechanism of white layer in the high-speed cutting of hardened steel under cryogenic liquid nitrogen cooling," *J Mater Process Technol*, vol. 302, p. 117469, Apr. 2022, doi: 10.1016/j.jmatprotec.2021.117469.
18. S. Liu, X. Wang, Z. Liu, Y. Wang, H. Chen, and P. Wang, "Microstructure and micromechanical properties evolution pattern of metamorphic layer subjected to turning process of carbon steel," *Appl Surf Sci*, vol. 608, p. 154679, Jan. 2023, doi: 10.1016/j.apsusc.2022.154679.
19. S. Padhan, S. R. Das, A. Das, M. S. Alsoufi, A. M. M. Ibrahim, and A. Elsheikh, "Machinability Investigation of Nitronic 60 Steel Turning Using SiAlON Ceramic Tools under Different Cooling/Lubrication Conditions," *Materials*, vol. 15, no. 7, p. 2368, Mar. 2022, doi: 10.3390/ma15072368.
20. A. R. C. Sharman, J. I. Hughes, and K. Ridgway, "An analysis of the residual stresses generated in Inconel 718™ when turning," *J Mater Process Technol*, vol. 173, no. 3, pp. 359–367, Apr. 2006, doi: 10.1016/j.jmatprotec.2005.12.007.
21. B. Li, S. Zhang, Q. Zhang, J. Chen, and J. Zhang, "Modelling of phase transformations induced by thermo-mechanical loads considering stress-strain effects in hard milling of AISI H13 steel," *Int J Mech Sci*, vol. 149, pp. 241–253, Jan. 2018, doi: 10.1016/j.ijmecsci.2018.10.010.